Insights into the Regulation of the Ryanodine Receptor: Differential Effects of Mg(2+) and Ca(2+) on ATP Binding

ARTICLE *in* BIOCHEMISTRY · SEPTEMBER 2006

Impact Factor: 3.02 · DOI: 10.1021/bi060623a · Source: PubMed

Insights into the Regulation of the Ryanodine Receptor: Differential Effects of Mg^{2+} and Ca^{2+} on ATP Binding†

José M. Dias,‡ Csaba Szegedi,§,|| Istvan Jóna,§ and Pia D. Vogel*,‡

Department of Biological Sciences, Southern Methodist University, 6501 Airline Road, Dallas, Texas 75275, MHSC, MMRI, and Department of Physiology, Univerity of Debrecen, H-4012 Debrecen, P.O. Box 22, Hungary, and Cell Physiological Research Group of the Hungarian Academy of Sciences, H-4012 Debrecen, P.O. Box 22, Hungary

Received March 29, 2006; Revised Manuscript Received April 27, 2006

ABSTRACT: Calcium ions are frequently used second messengers in most living organisms. Members of the family of ryanodine sensitive calcium channels (ryanodine receptors, RyRs) are responsible for many important Ca^{2+} signaling events in both excitable and nonexcitable cells. The biological activity of these membrane proteins is modulated and regulated by a great variety of different cellular and extracellular effectors, proteins, and small molecules. However, very little is still understood about how the modulators work on a molecular level. The very large size of more than 2 million Da per functional tetrameric RyR unit and its membrane association have made more detailed biochemical and structural analysis extremely challenging.

In this study, we have investigated the effects of the main cellular effectors of RyR,[1] Ca^{2+} and Mg^{2+}, on the properties for binding of the channel's third cellular modulator, ATP, to RyR. Employing an innovative approach using ESR spectroscopy and an ATP analogue that carries an ESR-active reporter group, spin-labeled ATP, we directly observed for the first time that a total of eight ATP sites exist on the tetrameric RyR1 purified from rabbit back muscle. We show that the number of ATP sites that are occupied by the ATP analogue and the respective dissociation constants directly depend on the presence and concentrations of Ca^{2+} and Mg^{2+} ions. The plant alkaloid ryanodine had no effect on ATP binding under activating Ca^{2+} conditions. Our findings will have strong implications for the current models for the regulation of cellular Ca^{2+} signaling.

Ryanodine receptors are homotetrameric protein complexes with a molecular mass of ∼560 kDa per subunit, forming the largest known ion channel protein. There are three different isoforms of this Ca channel protein that are found in different mammalian tissues. RyR1 is mostly located in the skeletal muscle; RyR2 is associated with heart muscle, and RyR3 is found in different cell types that do not necessarily constitute contractile cells (*1*). Although the Ca channel activity of the three different isoforms of RyR is highly regulated by many physiologically and pharmacologically important agents and proteins (*2*−*5*), it is assumed that Ca^{2+}, Mg^{2+}, and ATP are key cellular regulators of the channel (for a recent review, see ref *6*). A strong dependence of the channel opening events on different concentrations of either ion or both ions was observed (*7*−*13*). Isolated RyR1 was shown to be activated in the presence of 1 μM Ca^{2+} and inhibited in the presence of 1 mM cytoplasmic Ca^{2+} (*3*), while inhibition of RyR by Mg^{2+} may be the result of two independent mechanisms (*14*). It is believed that Mg^{2+} competes with Ca^{2+} for the activating sites (*15*) or, alternatively, that Mg^{2+} can bind to low-affinity, inhibitory, non-ion-selective sites that can also mediate Ca^{2+} inhibition of the channel (*15*, *16*). A reduced Mg^{2+} inhibition and increased Ca sensitivity (*5*) were found in malignant hypothermia, linking this important disease to a malfunctioning regulation of the ryanodine receptor (*17*).

ATP was also previously shown to strongly modulate the Ca^{2+} channel activities. Even in the absence of cytoplasmic, activating Ca^{2+} ions, ATP strongly activates RyR1. Full activation then results from the presence of both Ca^{2+} and ATP. The dissociation constants for ATP that have been reported previously (*10*, *11*, *15*, *18*) to be in the high micromolar and lower millimolar range will result in maximal RyR activation at cellular ATP concentrations of ∼8 mM in muscle cells (*19*). RyR2 from cardiac muscle is not activated by ATP to the same extent as RyR1 in the absence of Ca^{2+} (*20*, *21*), but ATP clearly aids the activation of RyR2 by Ca^{2+}. These different effects of adenine nucleotides in the cardiac muscle RyR are deemed to be part of the primarily important regulation events during contraction of the heart (*21*, *22*).

† This work was supported by a Beginning Grant-In-Aid from the American Heart Association, Texas Affiliate, and a grant from the Southern Methodist University Research Council to P.D.V. and a grant from OTKA K 61442 to I.J.

* To whom correspondence should be addressed: Department of Biological Sciences, Southern Methodist University, 6501 Airline Rd., Dallas, TX 75275. Telephone: (214) 768-1790. Fax: (214) 768-3955. E-mail: pvogel@mail.smu.edu.

‡ Southern Methodist University.

§ Univerity of Debrecen.

|| Cell Physiological Research Group of the Hungarian Academy of Sciences.

[1] Abbreviations: ESR, electron spin resonance spectroscopy; RyR, ryanodine sensitive Ca channel; SL-ATP, 2′,3′-(2,2,5,5-tetramethyl-3-pyrroline-1-oxyl-3-carboxylic acid ester) ATP, where 2′,3′ depicts a rapid equilibrium of the ester bond between the 2′ and 3′ positions of the ribose.

10.1021/bi060623a CCC: $33.50
Published on Web 07/15/2006

ESR spectroscopy employing spin-labeled nucleotide analogues was shown to be a powerful tool in studying structure, function, and binding characteristics of nucleotide binding enzymes and proteins (*23*−*30*). The affinity and stoichiometry for binding of spin-labeled (SL) substrate analogues to proteins can be directly determined under equilibrium conditions due to the fact that the signal shape of the ESR spectra of the protein-bound spin-labeled substrate differs significantly from that of the free substrate analogue. The respective experiments are designed to incrementally increase the amount of spin-labeled substrate at known protein concentrations. The signal amplitude of the high-field ESR signal of freely tumbling, non-protein-bound spin-labeled nucleotide in the presence of protein is then compared to the signal amplitude of the spin-labeled nucleotide in a standard curve that was obtained in the absence of protein. This technique is especially amenable to the study of membrane proteins, since light scattering effects that often influence other spectroscopic techniques, like fluorescence spectroscopy, do not influence the ESR signal. The technique can also be successfully applied in investigating enzymes with relatively weak substrate binding affinities, because the signal amplitude of the freely tumbling spin-labeled analogue is directly proportional to its concentration up to ~1 mM. One prerequisite of the ESR technique is that relatively high enzyme concentrations are needed to obtain high-quality ESR spectra that will allow the respective substrate binding curves to be derived. RyR1 used in this study was purified from rabbit back muscle, and the purification procedure was optimized to yield concentrations between 6 and 10 μM (10−20 mg/mL) of solubilized, biologically active protein that was more than 95% enriched.

EXPERIMENTAL PROCEDURES

Purification of RyR. RyR was purified from rabbit back muscles according to the original Meissner procedure (*31*) with some modifications. To obtain high protein concentrations of biologically active, pure RyR1 while retaining a relatively low overall viscosity of the protein solution, we solubilized the heavy sarcoplasmic reticulum vesicle preparations prepared as described in ref *31* at 7.5 mg/mL protein for 2 h at 4 °C. The solubilization buffer contained 30 mM PIPES/NaOH (pH 7.4), 1.5 M NaCl, 150 μM EGTA, 225 μM $CaCl_2$, 1.6% (w/v) CHAPS, 0.35% (w/v) phosphatidylcholine (100%), 0.35% (w/v) lysophosphatidylcholine, 1.5 mM DTT, and the usual protease inhibitors. Insoluble protein was removed by ultracentrifugation, and the supernatant was layered onto a 10 to 28% sucrose gradient generated in the same buffer. The RyR-containing fractions were extracted as described above, and an equal volume of buffer containing 40 mM PIPES/NaOH (pH 7.4), 2 M NaCl, 200 μM EGTA, and 300 μM $CaCl_2$ was added. The solution was concentrated at 4 °C in a Centricon Plus-20 device to 10−20 mg/mL. Aliquots (50 μL) were frozen and stored at −80 °C for single use in ESR experiments. Storage of the protein under such conditions was previously shown to keep the channel in a function-preserved tetrameric form that could be used for single-channel measurements (*11*). To stabilize the channel for the duration of the ESR experiments, we chose to directly use the aliquots that were concentrated as described above in the ESR experiments.

Determination of Ion Concentrations. All concentrations for free Ca^{2+}, free Mg^{2+}, or unchelated and chelated spin-labeled ATP were calculated using the *MAXC* algorithms as described previously (*32*). We assumed that the ion binding affinities of SL-ATP are identical or at least very similar to those of ATP. Due to our experimental setup, the concentration of the free ions and free and ion-complexed SL-ATP changed during the course of the titration experiments. The divalent ion concentrations given throughout this paper stand for representative upper and lower limits of concentrations during the experiments. Potential complex formation of ATP with Na^+ was not entered into the calculations since the Na^+ concentrations were essentially identical in the different sets of experiments.

Synthesis of SL-ATP. 2′,3′-(2,2,5,5-Tetramethyl-3-pyrroline-1-oxyl-3-carboxylic acid ester) ATP (SL-ATP) was synthesized essentially as described previously (*33*, *34*), except that the nucleotide analogue was purified using DEAE-A25 anion exchange chromatography and a linear gradient of 0−0.6 M triethylammonium bicarbonate buffer (pH 7.5) as described previously (*30*).

Routine Procedures. Protein concentrations were determined by a modified Lowry procedure (*35*) using bovine serum albumin as a standard. During this procedure, the proteins were precipitated using trichloroacetic acid in the presence of desoxycholate prior to addition of the color reagents. The denatured proteins were pelleted by centrifugation, leaving lipids, detergents, DTT, and other soluble components of the sucrose gradient in the supernatant. The supernatants were carefully removed. Thus, potential components from the sucrose gradient that might interfere with the color development of the Lowry reagents were efficiently eliminated prior to addition of the Lowry reagents. Protein purity was assessed using 6% SDS−polyacrylamide gel electrophoresis and was found to be >90%. Single-channel measurements were performed as described previously (*11*).

ESR Measurements. All ESR measurements were performed with a Bruker EMX 6/1 ESR spectrometer operating in the X-band mode, using a high-sensitivity cavity. The spectra were acquired at room temperature. The parameters were as follows: microwave frequency, 9.33 GHz; microwave power, 12.63 mW; modulation frequency, 100 kHz; modulation amplitude, 1 G; time constant, 10.40 ms; conversion time, 40.96 ms. The signal gain was adjusted to the different experimental conditions. Control experiments showed that the spin-label was not reduced by DTT during the time course of a typical experiment. The amount of protein-bound spin-labeled nucleotide was determined as the difference between the known total concentrations of spin-labeled nucleotide added to the ESR cuvette and the free spin-labeled nucleotide observed. The free nucleotide was assessed directly by comparing the signal amplitude of the high-field ESR signal of the unbound spin-labeled nucleotide to a standard curve of known concentrations of spin-labeled nucleotide that was generated under the same conditions in the absence of protein. Due to the high molecular weight of RyR combined with the high concentration of protein needed for the titration experiments, the viscosity of the protein-containing solution was increased when compared to that of the solution of the standard curve. This increased viscosity of the protein-containing solutions during a titration experiment led to a broadening of the ESR spectral lines, thereby

Table 1: Binding of Spin-Labeled ATP to RyR under Different Ionic Conditions[a]

experimental conditions	maximal binding of SL-ATP to RyR1 (mol/mol)	apparent K_d (μM)	R^2	reduced χ^2
2 mM EGTA (essentially no free divalent ions present)	7.6 ± 0.4	276 ± 30	0.98	0.07
<100 μM Ca^{2+} with or without 20 μM ryanodine	8.5 ± 0.5	171 ± 26	0.94	0.22
1.7−2 mM Mg^{2+}	8.9 ± 0.4	162 ± 30	0.95	0.28
1.5−2 mM Mg^{2+} with <100 μM Ca^{2+}	8.6 ± 0.5	91 ± 18	0.88	0.68
1.7−2 mM Ca^{2+}	4.2 ± 0.2	75 ± 16	0.87	0.15
1.9−2.1 mM Ca^{2+} with 1.7−2 mM Mg^{2+}	4.2 ± 0.08	50.4 ± 4.2	0.98	0.03

[a] Binding of SL-ATP to RyR was performed as described in Experimental Procedures. Maximal binding and apparent dissociation constants were determined by nonlinear curve analysis for a rectangular hyperbola. R^2 is the correlation coefficient of the fit, and reduced χ^2 as calculated by the fitting program represents the value for (data value minus function value)^2/(number of points minus number of parameters). A low value of reduced χ^2 indicates a good match between the data and the fitting model. Ion concentrations were calculated using the *Maxc* algorithm (*32*).

causing a decrease in signal amplitude. A decrease in signal amplitude, however, mimics the binding of the spin-labeled ATP to the protein and would result in an overestimation of the maximal binding stoichiometry. To correct for this phenomenon, we obtained sample standard curves in the presence of RyR that we had previously observed not to bind to SL-ATP, potentially due to minor damage during purification. In addition, we added a large excess of 10 mM ATP to the solution to outcompete any potential binding of SL-ATP to the channel. In Figure 1 of the Supporting Information, we present an overlay of the high-field ESR signals of free SL-ATP (125 μM) in the absence of protein (black line) and in the presence of "binding-incompetent" protein and 10 mM ATP (blue line) and of the "normal" binding-competent protein (red line). The protein concentrations were between 15 and 17 μM for the different experiments; the amount of added SL-ATP was identical in all three cases. Broadening of the line shape of the ESR signal and the decreased signal amplitude were observed in the presence of the binding-incompetent protein due to the increased viscosity of the solution (compare the blue line to the black line). An additional decrease in the signal amplitude (red line) that was observed when normal, functional RyR was incubated with SL-ATP (red line) was due to binding of SL-ATP to RyR and was concomitant with the appearance of ESR signals that correspond to the spectra of SL-ATP that was bound to RyR. These "bound signals" are distinctly different from those of free SL-ATP; for example, see Figure 2 of the Supporting Information. The numbers of moles of nucleotides bound per mole of RyR that are presented in this paper were corrected for the line broadening of the ESR spectra due to increased viscosity and represent "real" binding of SL-ATP to the channel.

The corrected numbers of moles of protein-bound SL-ATP per mole of protein were plotted over the concentration of free SL-ATP present in the experiment, and the results were fitted using the equation $y = P1 \times x/(P2 + x)$ for a rectangular hyperbola. P1 represents the maximum number of binding sites, and P2 represents the apparent equilibrium dissociation constant (K_d). Nonlinear curve fits were performed using Origin 7 (OriginLab Corp.). The data were not weighted. The reduced χ^2 for the individual fits and the correlation coefficients (R^2) for the fitted curves are given in Table 1. The reduced χ^2 as calculated by the fitting program represents the value for (data value minus function value)^2/(number of points minus number of parameters). A low value of reduced χ^2 indicates a good match between data and the fitting model.

RESULTS

SL-ATP as an Analogue of ATP for Binding to RyR1. Two different spin-labeled ATP analogues were tested with respect to their ability to bind to RyR1 that was isolated from rabbit back muscle. The two analogues contained the spin-label attached either to the C8 position (8-SL-ATP; see refs *28* and *29*) of the adenine or to the C2′ or C3′ position of the ribose (*23*−*27*, *30*, *33*, *34*). Only the analogue where the spin-label is attached to the ribose, 2′,3′-SL-ATP (SL-ATP), was observed to bind to RyR. The biological activity of SL-ATP was tested in single-channel measurements as described in ref *11*. The left panel of Figure 1 shows that the analogue stimulated RyR1 channel activity like normal ATP (right panel) in a concentration-dependent manner. Adding excess normal ATP to the SL-ATP-stimulated channel evoked an additional activating effect. Addition of ryanodine to the SL-ATP-activated channel produced the expected effects; i.e., ryanodine caused the channel to achieve a half-maximal opening in the presence of SL-ATP (data not shown). We should stress here that these are single-channel experiments and that one cannot expect each individual channel to be identical in activity to the next. In the example shown here, the two particular channels shown in Figure 1 had different starting P_o values, so the total values at different ATP or SL-ATP concentrations differ to some extent; what is important however, it that the overall trend in opening events is very similar. One also needs to consider that the fourth trace in the left panel represents a total of 500 μM SL-ATP in addition to the 1 mM ATP added, which explains the overall higher P_o observed in this experiment when compared to that in the experiment shown in the right-hand panel.

Binding of SL-ATP to RyR1 in the Presence of Activating Concentrations of Ca^{2+}. We demonstrated that SL-ATP readily bound to the purified, solubilized RyR using standardized ESR titration experiments. In these experiments, the concentration of freely tumbling SL-ATP in equilibrium with RyR-bound SL-ATP is directly deduced from its signal amplitude and compared to a standard curve obtained under the same conditions. The amount of RyR-bound SL-ATP was then calculated from the known protein concentration. The signal amplitude of the ESR signal of free SL-ATP was corrected for the increased viscosity of the sample solution due to the high protein concentration. This increase in viscosity caused an increase in the line width of the ESR signal and thereby resulted in a decreased signal amplitude, which mimicked binding of the probe to the protein (see Experimental Procedures and Figure 1 of the Supporting Information).

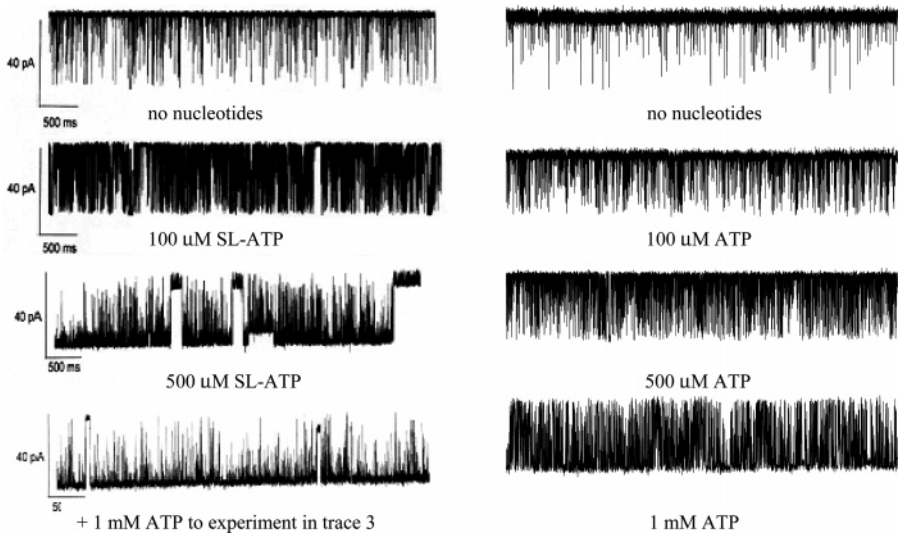

FIGURE 1: Single-channel measurements using SL-ATP. Representative current traces obtained at various SL-ATP and ATP concentrations in a medium of symmetrical 250 mM KCl and 20 mM PIPES (pH 7.4). The free calcium concentrations of 50 μM Ca^{2+}_{trans} and 472 nM Ca^{2+}_{cis} were adjusted using Ca-EGTA buffer. The holding potential was −60 mV; downward deflections represent the channel openings. Left: lane 1, no nucleotides present; lane 2, in the presence of 100 μM SL-ATP; lane 3, at 500 μM SL-ATP; and lane 4, after addition of 1 mM ATP to the mixture shown in lane 3. Right: lane 1, no nucleotides present; lane 2, in the presence of 100 μM ATP; lane 3, 500 μM SL-ATP; and lane 4, 1 mM ATP.

We observed that in the presence of activating concentrations of Ca^{2+} ions (≤100 μM), a total of eight SL-ATP molecules readily bound to RyR, both in the presence and in the absence of inhibitory concentrations of ryanodine (Table 1). The concentrations of free ions and free and ion-complexed SL-ATP were calculated using the *MAXC* algorithm (*32*) as described in Experimental Procedures. As an example of a representative binding curve, the results for binding of SL-ATP to RyR in the presence of an activating concentration of Ca^{2+} (<100 μM) and in the presence of 20 μM ryanodine (slightly superstoichiometric to the protein concentrations used for the experiment) are shown in Figure 2. Nonlinear hyperbolic curve analysis extrapolates to a maximum binding of 8.5 ± 0.5 mol/mol of nucleotide bound per RyR tetramer with a K_d of 171 ± 26 μM. Due to the relatively long measurement times required for ESR experiments and to ensure active RyR throughout the course of an experiment, all titration curves shown in this paper are composites of multiple independent experiments, using different purification batches of RyR. Experiments performed in the absence of ryanodine resulted in essentially the same binding stoichiometry and dissociation constant as in the presence of ryanodine (data not shown), indicating that binding of ryanodine and its effect on the channel activity were not linked to changes in ATP binding affinity and stoichiometry.

Binding of SL-ATP to RyR1 in the Absence of Divalent Ions. A similar binding stoichiometry of ~8 mol of ATP/RyR was observed also in the presence of 2 mM EGTA, which results in negligible concentrations of free Ca^{2+} (data not shown). Under these conditions, we calculated that SL-ATP was also not ion-chelated. Nonlinear curve analysis indicated a maximal binding of 7.6 ± 0.4 mol/mol and an increased K_d of 276 ± 30 μM. The experiments demonstrated that SL-ATP also bound to RyR in a non-metal-chelated form, albeit with a decreased affinity, and that binding of divalent ions to RyR is not needed for binding of SL-ATP to RyR. One representative set of ESR spectra that was

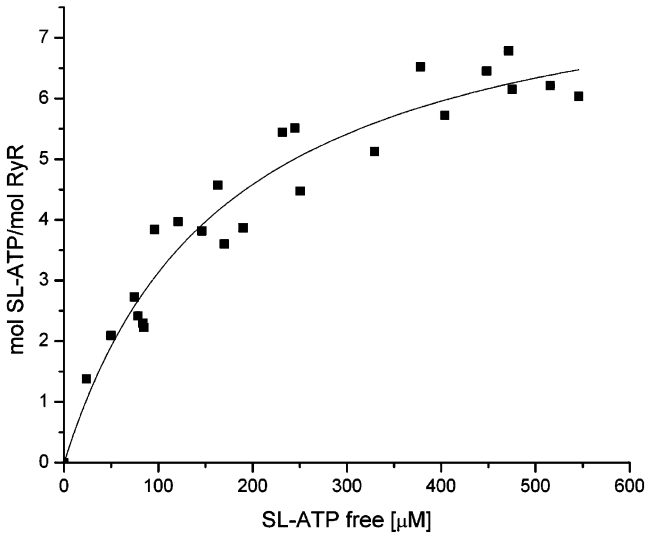

FIGURE 2: Titration of RyR with SL-ATP in the presence of activating Ca^{2+} and inhibitory ryanodine concentrations. Spin-labeled ATP was added stepwise to a solution containing 5−10 μM purified, solubilized RyR in the presence of 20 μM ryanodine and <100 μM Ca^{2+} (the concentration of free Ca^{2+} ions changed during the titration experiment due to chelating the ion to the ATP analogue). The number of RyR-bound SL-ATP molecules was determined by comparing the signal amplitude of the high-field ESR signal of the unbound spin-labeled ATP in the presence of RyR to that measured in a standard curve in the absence of RyR, but corrected for the increase in viscosity as described in Experimental Procedures. Nonlinear curve analysis determined a maximal binding of 8.5 ± 0.5 mol of SL-ATP/RyR and an apparent K_d of 171 ± 26 μM. Essentially the same values were obtained in the absence of ryanodine.

obtained under the conditions described here can be seen in Figure 2 of the Supporting Information. The spectra of the free, non-RyR-bound SL-ATP in the presence of RyR can be observed as the three relatively sharp lines in the middle of the spectra. The total concentration of SL-ATP added to this experiment was 80 μM. The spectra of the protein-bound SL-ATP can be observed concurrently, together with the spectra of the free component; however, the bound spectra

are much broader and less pronounced than those of the free components, which is typical for these experiments (*23*−*30*, *34*). These signals need to be re-recorded at a higher signal gain for visualization. The re-recorded bound spectra are shown in Figures 2−4 of the Supporting Information in the high- and low-field area of the spectra. The concentrations of total spin-label added to each experiment are given in the figure legends.

Binding of SL-ATP to RyR1 in the Presence of Inhibitory Concentrations of Mg^{2+}. In the presence of inhibitory concentrations of free Mg^{2+} (from 1.7 to 2 mM) and absence of free Ca^{2+} (with >2 mM EGTA), the binding curve for binding of SL-ATP to RyR extrapolates to a maximal binding of 8.9 ± 0.4 mol/mol with a dissociation constant of 162 ± 30 μM (data not shown, Table 1). The dissociation constant under these conditions is ∼1.7-fold lower than in the absence of divalent cations but ∼1.8-fold higher than in the co-presence of activating concentrations of Ca^{2+} (discussed below), indicating that Mg^{2+}-chelated ATP binds more tightly to RyR but that activating Ca ions further promote ATP binding.

Binding of SL-ATP to RyR1 in the Presence of Activating Concentrations of Ca^{2+} and Inhibitory Concentrations of Mg^{2+}. In the presence of inhibitory free Mg^{2+} concentrations (1.5−2 mM) and <100 μM free Ca^{2+}, which can be assumed to be borderline activating, binding of SL-ATP to RyR is tighter than in the presence of Mg ions alone. The binding curve shows an apparent K_d of 91 ± 18 μM and extrapolates to a maximum binding of 8.6 ± 0.5 SL-ATP molecules/RyR tetramer (data not shown, Table 1). The maximum concentration of non-ion-chelated SL-ATP in this experiment was ∼25 μM at the highest concentration of SL-ATP, strongly indicating that Mg^{2+}-chelated SL-ATP is the species that binds to the channel under these conditions. The binding affinity increased by >2.5-fold as compared to that of unchelated ATP (in the presence of 2 mM EGTA).

Binding of SL-ATP to RyR1 in the Presence of Inhibitory Concentrations of Ca^{2+}. Further titration experiments were performed in the presence of inhibitory amounts of free Ca^{2+} (1.7−2 mM). Under these conditions, ATP was calculated to be complexed almost completely to Ca^{2+}, and it can be assumed that Ca-chelated SL-ATP is the species that interacts with RyR. The experimental curve is shown in Figure 3. Nonlinear curve analysis shows a very tight binding constant of 75 ± 16 μM for binding of SL-ATP to RyR, ∼4-fold tighter than in the absence of free metal ions and lower also than in the experiments, where both Mg^{2+} and Ca^{2+} ions were present. Surprisingly, however, the maximal binding stoichiometry was observed to be only 4.2 ± 0.2. This experiment, combined with the previously described experiments, clearly demonstrates a direct effect of metal ions on the nucleotide accessibility of RyR, potentially as a result of a conformational transition that in return may induce or be responsible for the opening and closing events of the channel. One corresponding set of ESR spectra that was used to determine the binding of SL-ATP to RyR under the conditions described in the legend of Figure 3 can be seen in Figure 3 of the Supporting Information.

Binding of SL-ATP to RyR1 in the Presence of Inhibitory Concentrations of Mg^{2+} and Inhibitory Concentrations of Ca^{2+}. In separate experiments, 2 mM Mg^{2+} was added to the inhibitory Ca^{2+} concentrations that are described for the

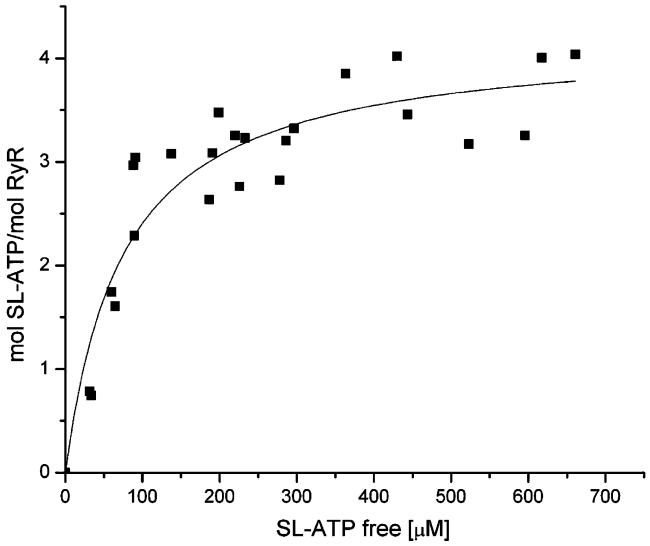

FIGURE 3: Titration of RyR with SL-ATP in the presence of inhibitory Ca^{2+} concentrations. The experiment was carried out as described in the legend of Figure 2. The concentration of EGTA in the experiment was 250 μM. Ca^{2+} concentrations were between 1.7 and 2 mM during the experiment. Nonlinear curve analysis showed a maximal binding of 4.2 ± 0.2 mol of SL-ATP/RyR and an apparent K_d of 75 ± 16 μM.

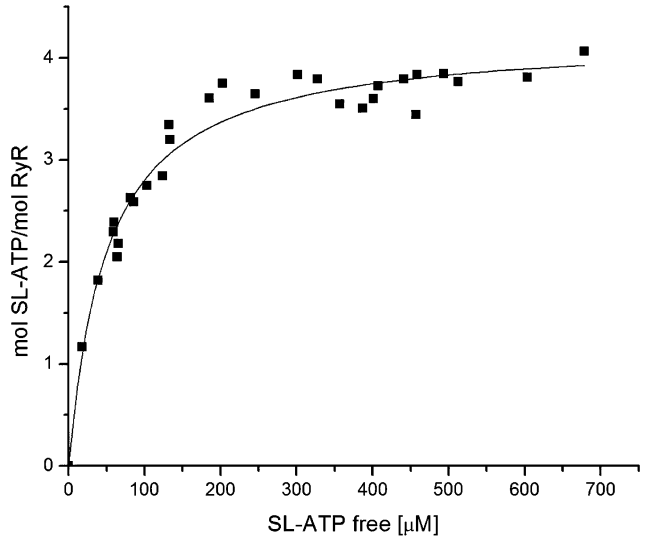

FIGURE 4: Titration of RyR with SL-ATP in the presence of inhibitory Ca^{2+} and inhibitory Mg^{2+} concentrations. The experiment was carried out as described in the legend of Figure 2. Ca^{2+} concentrations varied between 1.9 and 2.1 mM and Mg^{2+} concentrations between 1.7 and 2 mM. Nonlinear curve analysis resulted in a maximal binding of 4.2 ± 0.08 mol of SL-ATP/RyR and an apparent K_d of 50.4 ± 4.2 μM.

experiments shown in Figure 3. Again, the maximum binding stoichiometry found was 4.2 ± 0.08, and the K_d was determined to be 50.4 ± 4.2 μM for SL-ATP binding (Figure 4), indicating that the effects of inhibitory concentrations of Ca^{2+} on the binding stoichiometry and affinity of RyR could not be overcome by the addition of Mg^{2+} ions, which by themselves or in the presence of only small amounts of Ca^{2+} lead to full occupancy of all eight nucleotide binding sites of RyR. A corresponding set of ESR spectra that show the increase in the level of binding of SL-ATP to RyR is shown in Figure 4 of the Supporting Information.

In all the experiments described herein, the spin-labeled ATP that was bound to RyR could be completely displaced

upon addition of excess normal ATP (for example, see Figure 3 of the Supporting Information), demonstrating that binding of SL-ATP to RyR was indeed solely dependent on the ATP part of the analogue and did not arise from nonspecific interactions of the spin-label with the protein.

DISCUSSION

It has been reported that ATP can open the ryanodine sensitive Ca channel from skeletal muscle, RyR1, even under conditions where almost no free Ca^{2+} is present (*10*). Small amounts of cytosolic Ca^{2+} also activate the channel, while large amounts of Ca^{2+} are responsible for closing the channel (*3*), which may been explained by the presence of activating Ca^{2+} binding sites on RyR with a high Ca binding affinity and low-affinity, inhibitory Ca^{2+} binding sites. The role of Mg^{2+} and its function in RyR regulation are even more controversial. It has been suggested that Mg^{2+} ions may inhibit the channel by competing with the activating Ca binding sites and/or binding to non-ion-selective inhibitory sites (*15*−*17*). It was also shown earlier that magnesium inhibition of RyR was altered in the presence of ATP. While isolated RyR that was incubated with activating Ca^{2+} in the absence of ATP showed cooperativity of Mg-induced inhibition, no cooperativity was observed in the presence of cellular amounts of ATP (*11*).

In this paper, we show for the first time that these events may be linked and that the accessibility and occupation of the ATP binding sites on RyRs strongly depend on the presence and concentration of divalent ions and may be the common denominator for the different regulatory events. Using ESR spectroscopy and an ESR active analogue of ATP, we were able for the first time to directly assess binding of ATP to RyR under different ionic conditions. The differential effects of the divalent cations, Mg^{2+} and Ca^{2+}, are summarized in Table 1. A model depicted in Figure 5 recapitulates the overall effects of Mg^{2+} and Ca^{2+} ions on binding of ATP to the ryanodine receptor that were observed in the experiments described here and their potential relations to channel characteristics.

In this first direct measurement of binding of ATP to RyR1, we show that a total of eight nucleotide binding sites are located on RyR1 from rabbit skeletal muscle. The presence of two different ATP sites per RyR monomer had been proposed earlier by inferring ligand binding from functional studies. In competition experiments using the competitive inhibitor of ATP activation, adenosine, two different classes of ATP sites with similar K_d values were suggested to reside on RyR (*10*). In other studies, the biphasic activation of RyR in response to increasing ATP concentrations (*11*) also implied different classes of ATP sites on RyR.

Using ESR titration experiments, we showed in direct measurements that 8 mol of a spin-labeled ATP analogue readily bound to the RyR tetramer under certain conditions. We showed that a spin-labeled ATP analogue that carries the radical at the ribose of ATP is a suitable analogue of ATP in single-channel measurements (Figure 1). SL-ATP-dependent RyR1 activation was observed and was similar to activation by normal ATP. In the presence of 500 μM SL-ATP, considerable channel opening was observed in single-channel experiments (Figure 1, left panel), and titration experiments (depicted in Figure 2) showed that under similar

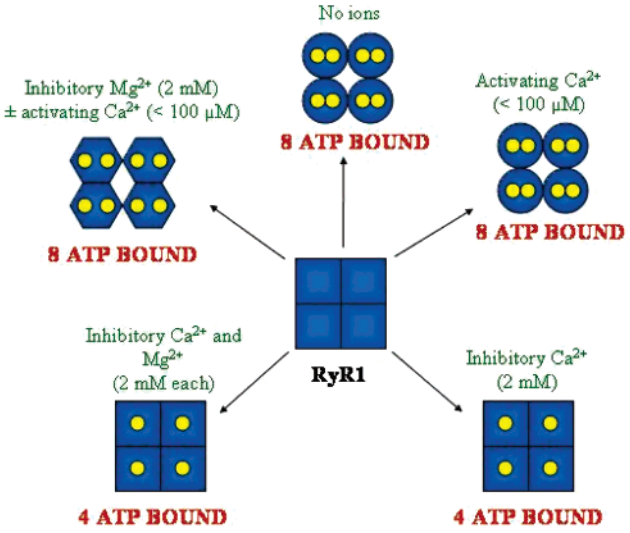

FIGURE 5: Schematic of the ion-dependent binding of SL-ATP to the ryanodine receptor and their potential role in channel opening. The circles represent the open channel. In the presence of activating Ca^{2+} concentrations, eight SL-ATP molecules are able to bind to RyR. A total of eight ATP molecules bound was observed also in the total absence of divalent ions. Under such conditions, functional studies by others have shown that the channel was activated for Ca^{2+} release. The hexagons represent the intermediate/primed channel. In the presence of inhibitory Mg^{2+} concentrations but in the presence of activating Ca^{2+} concentrations, again eight ATP molecules were able to bind to RyR. Although functional studies show that the channel is not opening under such ionic conditions, the data presented here may suggest that RyR may be primed by ATP binding for opening events. The squares represent the closed channel. In the presence of inhibitory Ca^{2+} concentrations, with or without Mg^{2+}, only four SL-ATP molecules bind to RyR, under conditions that were previously shown to cause the formation of a closed channel.

conditions almost all eight ATP sites were occupied by the ATP analogue. While it cannot be shown unequivocally at this time that full occupancy of all eight ATP sites is indeed essential for channel opening, the results from our experiments are suggestive of this possibility.

The two ATP sites that reside on each of the RyR monomers seem to be functionally different. In the absence of free divalent ions, which may not represent a physiologically relevant condition, all eight ATP sites on RyR are available for ATP binding and are occupied by SL-ATP with a dissociation constant which is in the high micromolar range (~300 μM). This implies, however, that even at drastically decreased cellular concentrations of divalent cations but a normal cellular ATP level, the channel can be fully occupied with eight ATP molecules, which may represent a channel that is "ready for activation" for Ca^{2+} release.

In the presence of activating concentrations of Ca^{2+}, at activating Ca^{2+} concentrations together with inhibitory Mg^{2+} concentrations, as well as in the presence of high, presumably inhibitory Mg^{2+} concentrations alone, all of these eight binding sites are also accessible and are occupied by ATP, even at ATP concentrations that are well below the normal cellular ATP levels. Except for the "no free metal ions" situation, the different scenarios potentially mimic different but essentially possible cellular states that may either prime the channel for subsequent opening events or have previously been shown or have been assumed to evoke channel opening events (low Ca^{2+} concentrations alone, or low Ca^{2+} concen-

trations in the presence of cellular levels of Mg^{2+}). The data presented here suggest that the occupation of eight ATP sites is linked to "open" or "opening" Ca^{2+} channels.

In the presence of high Ca^{2+} concentrations while the free Mg^{2+} concentration is low or in the presence of both high Ca^{2+} and high Mg^{2+} concentrations, only four of these ATP sites are accessible and occupied by ATP, even at high ATP concentrations. We speculate that this particular state of the channel may represent a fail-safe feedback reaction of the muscle that prevents continuous contraction after an excitation event. Our observation that only four of the ATP sites are accessible under these conditions suggests that even in the presence of high Mg^{2+} and high ATP concentrations, which would allow fast Ca^{2+} export by the SERCA ATPase, this feedback inhibition remains intact. Similar calcium-induced inactivation effects were reported previously (*36*).

There are potentially two alternative explanations for the differential binding of four or eight ATP molecules to RyR in the presence or absence of Mg^{2+} and/or Ca^{2+}. (1) The channel assumes different conformations (which may relate to open or closed in function) in the presence or absence of Ca^{2+} or Mg^{2+}. This may then result in different accessibilities for the binding of ATP, leading to maximal binding of either four or eight ATP molecules. Binding ATP may then stabilize the open or closed conformation. Alternatively, the opening or closing events may be caused by conformational changes that resulted from ATP binding. (2) A second possibility would be that the different Mg^{2+} or Ca^{2+} complexes of ATP simply result in different binding affinities for RyR. We believe the events proposed in the first alternative to be more likely, especially since almost equimolar, high concentrations of Mg^{2+} and Ca^{2+} result in maximal binding of only four ATP molecules per RyR (see Figure 4) while eight SL-ATP molecules bind in the absence of divalent cations. We assume that at equimolar Mg^{2+} and Ca^{2+} concentrations, ATP would be complexed to almost equal amounts with either Mg^{2+} or Ca^{2+}, which should result in mixed populations of binding affinities and binding stoichiometries. We therefore hypothesize that the occupancy of only four ATP sites per RyR tetramer is most likely directly linked to the formation of the closed state of the channel. This may occur under physiological conditions potentially as the result of a fatigued muscle at very low cellular ATP concentrations (not enough ATP to fill the "activating" sites), at very low Mg^{2+} concentrations due to the cellular imbalance of ions (K_d for ATP binding was increased by ~6-fold to approximately 300 μM in the absence of ions as compared to both high Mg^{2+} and high Ca^{2+} concentrations), or as a result of an activated muscle at high Ca^{2+} concentrations to prevent further excitation.

The effects of the plant alkaloid ryanodine on the activity of RyR do not seem to be linked to the binding of ATP to RyR, which may suggest a different regulation mechanism for this type of external modulator. We need to state at this point, though, that we have so far investigated only the effect of ryanodine on ATP binding at activating Ca^{2+} concentrations. Ryanodine has been shown to strongly affect the regulatory effects of intracellular modulators; i.e., RyR in the presence of ryanodine seems to be insensitive or less sensitive to cytoplasmic and/or luminal Ca^{2+} and nucleotides (*37*−*39*) as well as inhibitory effects evoked by high Mg^{2+} concentrations or low pH (*40*−*42*). Studying the characteristics of binding of ATP to ryanodine-modified RyR under different ionic conditions will be of great interest, as will correlating those to functional assays.

In this paper, we show for the first time and in direct measurements that ryanodine receptors from skeletal muscle contain a total of eight nucleotide binding sites that can be divided into two different classes. We hypothesize that the binding of a total of eight ATP molecules per RyR tetramer either stabilizes an open channel conformation or primes the channel for opening events, while binding of ATP to only four of the sites seems to correlate to conditions that were shown to cause formation of a closed channel. Whether the eight sites found under low-Ca^{2+} conditions (potentially activating) include the four sites found under high-Ca^{2+} conditions (inhibitory) or whether those sites are unrelated is unclear. Experiments aimed at identifying the respective ATP binding sites using photoaffinity nucleotide probes and subsequent analysis of the labeled peptides are underway in our laboratory. Linking the occupancy of the specific ATP sites to specific regulatory events of the receptor, i.e., linking the occupancy to functional studies, will give unprecedented insight into the mechanism of this physiologically and pharmacologically important protein family.

ACKNOWLEDGMENT

We thank J. Zirkel (Lipoid GmbH, Ludwigshafen, Germany) for the generous gift of 100% PC and 100% lyso-PC. We also thank J. G. Wise for discussion and critical reading of the manuscript.

SUPPORTING INFORMATION AVAILABLE

ESR spectra that correspond to the titration experiments shown in Figures 2−4, as well as the correction of the signal amplitudes for the viscosity of the standard curves that were used for quantification of the protein-bound spin-labeled ATP. This material is available free of charge via the Internet at http://pubs.acs.org.

REFERENCES

1. Ogawa, Y. (1994) Role of ryanodine receptors, *Crit. Rev. Biochem. Mol. Biol. 29*, 229−274.
2. Coronado, R., Morrissette, J., Sukhareva, M., and Vaughan, D. M. (1994) Structure and function of ryanodine receptors, *Am. J. Physiol. 266*, C1485−C1504.
3. Meissner, G., (1994) Ryanodine receptor/Ca^{2+} release channels and their regulation by endogenous effectors, *Annu. Rev. Physiol. 56*, 485−508.
4. Zucchi, R., and Ronca-Testoni, S. (1997) The sarcoplasmic reticulum Ca^{2+} channel/ryanodine receptor: Modulation by endogenous effectors, drugs and disease states, *Pharmacol. Rev. 49*, 53−98.
5. Meissner, G. (2002) Regulation of mammalian ryanodine receptors, *Front. Biosci. 7*, 2072−2080.
6. Laver, D. R. (2005) Coupled calcium release channels and their regulation by luminal and cytosolic ions, *Eur. Biophys. J. 34*, 359−368.
7. Smith, J. S., Coronado, R., and Meissner, G. (1985) Sarcoplasmic reticulum contains adenine nucleotide-activated calcium channels, *Nature 316*, 446−449.
8. Stange, M., Xu, L., Balshaw, D., Yamaguchi, N., and Meissner, G. (2003) Characterization of recombinant skeletal muscle (Ser-2843) and cardiac muscle (Ser-2809) ryanodine receptor phosphorylation mutants, *J. Biol. Chem. 278*, 51693−51702.
9. Butanda-Ochoa, A., Hojer, G., and Diaz-Munoz, M. (2003) Modulation of the skeletal muscle Ca^{2+} release channel/ryanodine receptor by adenosine and its metabolites: A structure−activity approach, *Bioorg. Med. Chem. 11*, 3029−3037.

10. Laver, D. R., Lenz, G. K. E., and Lamb, G. D. (2001) Regulation of the calcium release channel from rabbit skeletal muscle by the nucleotides ATP, AMP, IMP and adenosine, *J. Physiol. 537*, 763−778.
11. Jona, I., Szegedi, C., Sarkozi, S., Szentesi, P., Csernoch, L., and Kovacs, L. (2001) Altered inhibition of the rat skeletal ryanodine receptor/calcium release channel by magnesium in the presence of ATP, *Pfluegers Arch. 441*, 729−738.
12. Fill, M., and Copello, J. A. (2002) Ryanodine receptor calcium release channels, *Physiol. Rev. 82*, 893−922.
13. Dulhunty, A. F., Laver, D., Curtis, S. M., Pacr, S., Haarmann, C., and Gallant, E. M. (2001) Characteristics of irreversible ATP activation suggest that native skeletal ryanodine receptors can be phosphorylated via an endogenous CaMKII, *Biophys. J. 81*, 3240−3252.
14. Laver, D. R., Baynes, T. M., and Dulhunty, A. F. (1997) Magnesium inhibition of ryanodine-receptor calcium channels: Evidence for two independent mechanisms, *J. Membr. Biol. 156*, 213−229.
15. Meissner, G. (1986) Ryanodine activation and inhibition of the Ca^{2+} release channel of sarcoplasmic reticulum, *J. Biol. Chem. 261*, 6300−6306.
16. Soler, F., Fernandez Belda, F., and Gomez Fernandez, J. C. (1992) The Ca^{2+} release channel in junctional sarcoplasmic reticulum: Gating and blockade by cations, *Int. J. Biochem. 24*, 903−909.
17. Laver, D. R., Owen, V. J., Junankar, P. R., Taske, N. L., Dulhunty, A. F., and Lamb, G. D. (1997) Reduced inhibitory effect of Mg^{2+} on ryanodine receptor-Ca^{2+} release channels in malignant hyperthermia, *Biophys. J. 73*, 1913−1924.
18. Meissner, G. (1984) Adenine nucleotide stimulation of Ca^{2+}-induced Ca^{2+} release in sarcoplasmic reticulum, *J. Biol. Chem. 259*, 2365−2374.
19. Godt, R. E., and Maugham, D. W. (1988) On the composition of the cytosol of relaxed skeletal muscle of the frog, *Am. J. Physiol. 254*, C591−C604.
20. Meissner, G., Rousseau, E., Lai, F. A., Liu, Q. Y., and Anderson, K. A. (1988) Biochemical characterization of the Ca^{2+} release channel of skeletal and cardiac sarcoplasmic reticulum, *Mol. Cell. Biochem. 82*, 59−65.
21. Kermode, H., Williams, A. J., and Sitsapesan, R. (1998) The interactions of ATP, ADP, and inorganic phosphate with the sheep cardiac ryanodine receptor, *Biophys. J. 74*, 1296−1304.
22. Ching, L. L., Williams, A. J., and Sitsapesan, R. (1999) AMP is a partial agonist at the sheep cardiac ryanodine receptor, *Br. J. Pharmacol. 127*, 161−171.
23. Vogel, P. D., Nett, J. H., Sauer, H. E., Schmadel, K., Cross, R. L., and Trommer, W. E. (1992) Nucleotide binding sites on mitochondrial F1-ATPase. Electron spin resonance spectroscopy and photolabeling by azido-spin-labeled adenine nucleotides support an adenylate kinase-like orientation, *J. Biol. Chem. 267*, 11982−11986.
24. Burgard, S., Nett, J. H., Sauer, H. E., Kagawa, Y., Schäfer, H.-J., Wise, J. G., Vogel, P. D., and Trommer, W. E. (1994) Effects of magnesium ions on the relative conformation of nucleotide binding sites of F1-ATPases as studied by electron spin resonance spectroscopy, *J. Biol. Chem. 269*, 17815−17819.
25. Lösel, R. M., Erbse, A. H., Nett, J. H., Wise, J. G., Berger, G., Girault, G., and Vogel, P. D (1996) Investigating the Structure of Nucleotide Binding Sites on the Chloroplast F_1-ATPase Using ESR Spectroscopy, *Spectrochim. Acta, Part A 52*, 73−83.
26. Burgard, S., Harada, M., Kagawa, Y., Trommer, W. E., and Vogel, P. D. (2003) Association of α-subunits with nucleotide-modified β-subunits induces asymmetry in the catalytic sites of the F1-ATPase $\alpha_3\beta_3$-hexamer, *Cell Biochem. Biophys. 39*, 175−181.
27. Haller, M., Hoffmann, U., Schanding, T., Goody, R. S., and Vogel, P. D. (1997) Nucleotide hydrolysis-dependent conformational changes in p21(ras) as studied using ESR spectroscopy, *J. Biol. Chem. 272*, 30103−30107.
28. Neuhofen, S., Theyssen, H., Reinstein, J., Trommer, W. E., and Vogel, P. D. (1996) Nucleotide binding to the heat-shock protein DnaK as studied by ESR spectroscopy, *Eur. J. Biochem. 240*, 78−82.
29. Guhr, P., Neuhofen, S., Coan, C., Wise, J. G., and Vogel, P. D. (2002) New aspects on the mechanism of GroEL-assisted protein folding, *Biochim. Biophys. Acta 1596*, 326−335.
30. Delannoy, S., Urbatsch, I. L., Tombline, G., Senior, A. E., and Vogel, P. D. (2005) Nucleotide binding to the multidrug resistance P-glycoprotein as studied by ESR spectroscopy, *Biochemistry 44*, 14010−14019.
31. Lai, F. A., and Meissner, G. (1990) Structure of the calcium release channel of skeletal muscle sarcoplasmic reticulum and its regulation by calcium, *Adv. Exp. Biol. 269*, 73−77.
32. Patton, C., Thompson, S., and Epel, D. (2004) Some precautions in using chelators to buffer metals in biological solutions, *Cell Calcium 35*, 427−431.
33. Streckenbach, B., Schwarz, D., and Repke, K. H. R. (1980) Analysis of phosphoryl transfer mechanism and catalytic centre geometries of transport ATPase by means of spin-labelled ATP, *Biochim. Biophys. Acta 601*, 34−46.
34. Vogel-Claude, P., Schäfer, G., and Trommer, W. E. (1988) Synthesis of a Photoaffinity-Spin-Labeled Derivative of ATP and its First Application on F_1-ATPase, *FEBS Lett. 227*, 107−109.
35. Peterson, G. L. (1977) A simplification of the protein assay method of Lowry et al. which is more generally applicable, *Anal. Biochem. 83*, 346−356.
36. Szentesi, P., Kovacs, L., and Csernoch, L. (2000) Deterministic inactivation of calcium release channels in mammalian skeletal muscle, *J. Physiol. 528*, 447−456.
37. Rousseau, E., Smith, J. S., and Meissner, G. (1987) Ryanodine modifies conductance and gating behavior of single Ca^{2+} release channel, *Am. J. Physiol. 253*, C364−C368.
38. Laver, D. R., Roden, L. D., Ahern, G. P., Eager, K. R., Junankar, P. R., and Dulhunty, A. F. (1995) Cytoplasmic Ca^{2+} inhibits the ryanodine receptor from cardiac muscle, *J. Membr. Biol. 156*, 213−229.
39. Laver, D. R., O'Neill, E. R., and Lamb, G. D. (2004) Luminal Ca^{2+}-regulated Mg^{2+} inhibition of skeletal RyRs reconstituted as isolated channels or coupled clusters, *J. Gen. Physiol. 124*, 741−758.
40. Masumiya, H., Li, P., Zhang, L., and Chen, S. R. (2001) Ryanodine sensitizes the Ca^{2+} release channel (ryanodine receptor) to Ca^{2+} activation, *J. Biol. Chem. 276*, 39727−39735.
41. Ma, J., and Zhao, J. (1994) Highly cooperative and hysteretic response of the skeletal muscle ryanodine receptor to changes in proton concentrations, *Biophys. J. 67*, 626−633.
42. Laver, D. R., Eager, K. R., Taoube, L., and Lamb, G. D. (2000) Effects of cytoplasmic and luminal pH on Ca^{2+} release channels from rabbit skeletal muscle, *Biophys. J. 78*, 1835−1851.

BI060623A